Biogeochemistry (2024) 167:1491–1510
https://doi.org/10.1007/s10533-024-01178-4

Calcium sorption and isotope fractionation in *Bacillus subtilis* and *Pseudomonas aeruginosa*

N. Nuvoli · A. D. Schmitt · S. Gangloff · V. A. Geoffroy

Received: 20 September 2023 / Accepted: 3 September 2024 / Published online: 23 October 2024

Abstract Bacteria are a key component of the critical zone, because of their role in the nutrient availability for the vegetation. There is still little knowledge on the direct role of bacteria on Ca storage/leaching in soils while it is an essential macronutrient for vegetation growth. In recent years, Ca stable isotopes have shown their potential in understanding the Ca biogeochemical cycle. Preliminary studies highlighted that in the presence of soil bacteria, the plant uptake of nutrients is increased due to the mineral bioweathering. Moreover, Ca isotope signatures of nutrient media also showed differences between growth experiments in batch in the presence and absence of bacteria. In this study, the focus is to verify if Ca adsorption and incorporation into/onto bacterial strains induce such isotopic fractionation. Batch experiments were carried out on *Pseudomonas aeruginosa* (a Gram-negative bacterium) and on the vegetative and sporulated forms of *Bacillus subtilis* (a Gram-positive bacterium). These experimentations showed that: (i) no observable isotopic fractionations were induced during calcium/bacteria contact for all experimental parameters (pH, kinetic, bacterial cell number, interaction time, dead/alive bacteria); (ii) Ca was mainly stored in the bacterial cell wall compartments. On the other hand, significant Ca isotopic differences between the spores and the sporulation medium ($\Delta^{44/40}Ca_{spores–sporulation\ medium}$ ranging from -0.53 to $-1.15‰$), suggest isotopic fractionation during the sporulation process, likely occurring during the attachment of Ca to carboxyl acid groups as calcium chelates with dipicolinic acid. The absence of Ca isotope fractionation during Ca sorption on vegetative and sporulated bacteria via passive channels indicates that the tested bacteria's contribution to the Ca biogeochemical cycle is indirect primary enhancing bioweathering and Ca bioavailability for vegetation. If confirmed by further studies, only the sporulation mechanisms itself may directly impact the Ca biogeochemical cycle.

Keywords Ca isotopes · Adsorption · Incorporation · Bacteria · Sporulation

Responsible Editor: Steven J. Hall

Supplementary Information The online version contains supplementary material available at https://doi.org/10.1007/s10533-024-01178-4.

N. Nuvoli (✉) · A. D. Schmitt · S. Gangloff
ITES, UMR 7063, CNRS, ENGEES, University of Strasbourg, Strasbourg, France
e-mail: n.nuvoli@unistra.fr

A. D. Schmitt
e-mail: adschmitt@unistra.fr

S. Gangloff
e-mail: sgangloff@unistra.fr

V. A. Geoffroy
BSC, UMR 7242, CNRS, University of Strasbourg, Strasbourg, France
e-mail: valerie.geoffroy@unistra.fr

Introduction

Unlike other macronutrients, such as nitrogen (N) or phosphorus (P), there are fewer studies concerning calcium (Ca), its dynamics in soils, and its availability to plants. Calcium is an essential nutrient with significant physiological and structural functions in plant metabolism (Marschner et al. 1999). Additionally, due to its divalent charge, and reduced hydration, it exhibits strong adsorption onto clay minerals and humic acids compared to other metal cations (Likens et al. 1998) and can promote persistent soil organic matter (Shabtai et al. 2023). It also serves as a vital metal for microorganisms engaged in cellular metabolism (Lovley and Lloyd 2000). Passive adsorption enables its bioaccumulation, independent of metabolism, onto bacterial membranes. Furthermore, it can passively diffuse into cells or be transported within cells, in an energy-dependent pathway (Haferburg and Kothe 2007). This element also assumes significance in sporulated bacteria, where the spore imparts heightened resistance to thermal, radiation, or pH-related environmental stresses. Notably, calcium forms a complex with dipicolinic acid, ensuring DNA stabilization and maintaining the dehydrated state of spores (Paidhungat and Setlow 2000; Setlow et al. 2006). The ubiquity of microorganisms in substantial quantities—bacterial or fungal—in natural environments gives rise to diverse metabolites. These metabolites possess properties that influence nutrient availability (Barnes and Nierzwicki-Bauer 1997) which is also enhanced by mineral solubilizing microorganisms (Blum et al. 2003; Matlakowska et al. 2012; Ortega-Morales et al. 2016).

Nevertheless, the implications of these biotic processes are not yet fully documented, particularly within the global biogeochemical cycles of elements such as calcium. It is crucial to consider the processes occurring at the cell wall/medium interface and the roles of highly reactive extracellular polymeric substances (EPS) produced in biofilm microbial communities and metabolism (efflux, internalization). The distinct roles of various biological agents and their metabolites in establishing biogeochemical alteration balances, including removing nutrients by living organisms, remain poorly understood (e.g., Blum et al. 2002).

In recent years, stable calcium isotopes have demonstrated their potential in elucidating processes at the soil–water-plant interface. For instance, the utilization of calcium isotopes to study biogeochemical calcium cycling in the critical zone has unveiled isotopic fractionations linked to both biotic factors (such as root uptake, intra-plant translocation, and vegetation recycling) and abiotic factors (including precipitation through secondary minerals, adsorption onto clay minerals, and manganese oxides) (Cobert et al. 2011a; Schmitt et al. 2013, 2017, 2023; Gussone et al. 2016; Brazier et al. 2019, 2020; Griffith et al. 2020 and references therein). Nevertheless, little is known on isotopic fractionation processes induced by bacteria. Preliminary microcosm results suggested that bacteria could influence the Ca isotopic signatures of soil-vegetation systems by dissolving Ca from apatite (Cobert et al. 2011a). In a forested watershed, calcium isotopes have been suggested to provide evidence for the role of bacteria in weathering apatite (respectively litterfall) during anoxic (respectively oxic) conditions (Gangloff et al. 2014; Griffith et al. 2020).

The objectives of the present study are:

(1) Gain insights into the interaction between calcium and bacteria and delineate the extent of adsorption (on solid surfaces) and absorption (active or passive incorporation into cells) in calcium storage.
(2) Investigate the presence of calcium isotopic fractionation associated with adsorption/incorporation onto/in cells and spores, along with potential controlling parameters (such as available calcium quantity, pH, contact duration, bacterial biomass, or membrane surface characteristics—Gram-positive, Gram-negative, spore).
(3) Specify the storage compartments of calcium during adsorption/incorporation into bacterial cells and identify the pertinent functional groups involved.
(4) Discuss the implication for the Ca biogeochemical cycle

To do this, were carried out on a spore-forming Gram-positive bacterium, *Bacillus subtilis*, and a Gram-negative bacterium, *Pseudomonas aeruginosa,* that produces siderophores, two bacteria chosen for their different surface chemical properties. Gram-negative bacteria surround their cytoplasmic membrane with a peptidoglycan cell wall and an outer membrane with an outer leaflet composed of lipopolysaccharide

while Gram-positive bacteria lack an outer membrane but are surrounded by layers of peptidoglycan many times thicker than is found in the Gram-negatives (Beveridge 1999).

Materials and methods

The microbiological aspects of the following experiments were conducted at the Biotechnology and cell signalling (BSC) laboratory, University of Strasbourg, located in Illkirch, France. The geochemical aspects were undertaken at the Cortecs-Pacite platform of the University of Strasbourg, located at the Institut Terre Environnement Strasbourg (ITES) in Strasbourg, France.

Preparation of solutions and culture medium

The Ca solutions used for the experiments were derived from hydrated calcium nitrate powder ($Ca(NO_3)_2$–4 H_2O) sourced from Alfa Aesar Puratronic® with a purity level of 99.9995%. The powder was dissolved in ultra-pure water, and the pH of the resulting solutions was subsequently adjusted as needed, employing 0.025 N HNO_3 and 0.1 N NaOH solutions.

The succinate culture medium is an iron-poor minimum synthetic medium modified from the original succinate (Composition in g/L 3.72 g K_2HPO_4,$3H_2O$, 1.50 g KH_2PO_4, 0.10 g $MgSO_4$,$7H_2O$, 0.50 g $(NH_4)_2SO_4$, 2.00 g succinic acid, 1.55 g NaOH, $[Ca]_{succinate} < 2.5 \times 10^{-2}$ µg/ml). The medium was filter sterilized with a 0.22 µm PES membrane, a commonly used method for the physical removal of microorganisms (Stericup® Air filter Unit, Merck). The sporulation medium was prepared using (for 1 l): 2.4 g meat extract, 2.4 g peptone, 1.2 g NaCl, 0.03 g KH_2PO_4, 13 g agar and distilled water. The medium was sterilized by heat treatment with an autoclave.

Bacterial culture conditions

Bacillus subtilis (ATCC 6633), a Gram-positive bacterium, and *P. aeruginosa* (ATCC 15692), a Gram-negative bacterium, were selected for this study due to their soil prevalence and ease of cultivation. *Bacillus* and *Pseudomonas* ubiquitously occur in natural environments and are two of the most intensively studied bacterial genera in the soil. They are often co-isolated from environmental samples (Spiers et al. 2000; Lyng and Kovacs 2023). These two bacteria share similar culture media and physicochemical growth conditions, including temperature, duration, and shaking conditions. For preculture, bacteria were grown in sterile 50 mL Falcon™ tubes containing 10 mL of sterile lysogeny broth (LB) medium. Incubation was carried out under aerobic conditions at 30 °C and 220 rpm for 18–24 h. After the overnight LB incubation, cells were centrifuged at 9871×*g* for 5 min and washed twice with 7 ml of sterile modified succinate medium. Subsequently, the pellets were re-suspended in 8 ml of sterile modified succinate medium, and 1 ml of this bacterial suspension was introduced into 50 ml Falcon™ tubes containing 24 ml of modified succinate medium. Incubation at 30 °C with shaking at 220 rpm was sustained for 24 h. This protocol induces nutrient deprivation, particularly a calcium deficiency in the bacteria, setting the ideal conditions for characterizing calcium adsorption/absorption.

Post-culture, the cells were pelleted by centrifugation at 9871×*g* for 5 min, washed twice with 7 ml of sterile modified succinate medium, and adjusted to an OD_{600nm} of 0.5 or 1 according to the experiment. An OD_{600nm} equal to 0.5 corresponds to ~ 2×10^9 CFU/ml (colony forming unit/ml) for *P. aeruginosa*, ~ 5×10^7 CFU/ml for vegetative *B. subtilis* and 2×10^7 CFU/ml for *B. subtilis* spores. In this study, we decided to set the OD_{600nm} value rather than the number of CFU in order to obtain similar microbial biomass from one bacterium to another since the size of the bacteria is not the same (respectively 2–4 µm by 0.5–2 µm, 1.5–3 µm by 0.3–0.8 µm and Ø1 µm, for *B. subtilis, P. aeruginosa* and *B. subtilis* spore respectively).

Bacillus subtilis was routinely cultivated for 24 h at 30 °C with continuous shaking at 220 rpm in LB medium. The sporulation agar medium contained within Roux bottles was inoculated with the *B. subtilis* LB pre-culture. These Roux bottles, provide a large surface for the microorganisms to grow, were then incubated at 37 °C for at least 1 week. The medium surface was washed off to harvest the cells using sterile physiological water. The resulting suspension was stored at 4 °C. Before usage, the spores were subjected to a heat treatment in a water bath at 80 °C for 20 min to eliminate potential vegetative cells. Subsequently, the spores underwent two cycles

of washing with filter-sterilized pure water and were subjected to centrifugation at 9871×*g* for 5 min. Cell suspensions were adjusted to OD_{600nm} values ranging from 0.5 to 4.5 according tothe experiments.

Adsorption experiments and samples digestion

Each batch adsorption experiment involved between 2 and 4 replicates. They were conducted as a function of Ca concentration (0.5 to 5 µg/mL), pH (5 to 7, adjusted by the addition of 5×10^{-2} N HNO_3 or 5×10^{-3} N NaOH solutions, and chosen because they aligned with an optimal range for microbial activity and nutrient availability in soils (Vammechelen et al. 1997), bacterial biomass ($OD_{600nm}=0.5$ or 1 for experiments with vegetative bacteria and $OD_{600nm}=0.5$ to 4.5 for experiments with spores with a constant calcium solution/bacteria suspension ratio equal to 1. The chosen condition for spore experiments (Ca concentration (1.6 µg/ml) and pH (5.6)) enable comparison with results obtained for vegetative bacteria. The various cell concentrations ranging from OD_{600nm} equal to 0.5 to 4.5 allow us to obtain a sufficiently high spore/Ca ratio for maximum Ca adsorption. To investigate how protonophores on the cell membrane could affect the Ca absorption, bacterial cells were incubated with 200 µM of CCCP (Carbonyl Cyanide m-Chlorophenylhydrazone), which is known as a proton motive force inhibitor of the inner membrane and therefore abolishes energy dependent uptake by bacteria. The activity of CCCP as a protonophore reversibly binds protons (H^+) and transports them across the cell membrane, leading to membrane depolarization, eradication of the electrochemical concentration gradient and reduced ATP production by ATP synthase (Ni et al. 2016; Plášek et al. 2017; Ruas et al. 2018). As a consequence, the uptake of Ca corresponds to diffusion across the membrane via porins or bound at the cell surfaces (Braud et al 2009). The CCCP experiments were conducted at pH 5.6 with an initial Ca concentration of 1.6 µg/ml and a contact time of 2 h. Bacteria/spores suspensions were centrifuged at 9871×*g* for 10 min, and the supernatants were discarded. Then, calcium solution was added to each centrifugation tube. The tubes were placed on an SB3 StuartTM rotator shaker at 40 rpm for agitation. After shaking, the tubes were centrifuged at 9871×*g* for 10 min, and the supernatants were filter sterilized using syringes and 0.22 µm cellulose acetate membrane filters conditioned with 18 mQ ultra-pure water, that do not cause any elemental concentration variation or isotope fractionation. To mineralize the bacteria, 3–5 ml of 6 N HCl were added to the polypropylene tubes, which were placed on the rotator shaker for agitation (overnight at 220 rpm). After this step, the content of these tubes was transferred to Savillex™ beakers, and two washes of the polypropylene tubes were operated, using 3–5 ml of 6 N HCl, to transfer the remaining material in the Savillex™ beakers to avoid losses. The samples were heated at 70 °C for 1 h and then evaporated. After evaporation, 1 ml of distilled HNO_3 and 0.2 ml of suprapure H_2O_2 were added to the samples, which were heated for one night and then evaporated. After this, 10 ml of 0.25 N HNO_3 were added to the Savillex™ beakers, heated at 70 °C for 1 h, and then transferred in 15 ml Falcon™ tubes. In the subsequent sections of the manuscript LAA and BAA refer to the liquid and bacteria after adsorption, respectively. IS represents the initial solution.

Cell fractionation experiments

Two or three replicates were carried out of each of the different treatments of each experiment.

Pseudomonas aeruginosa

The cell fractionation protocol (Fig. 1) is derived from a procedure originally employed in the BSC laboratory (Guillon et al. 2012; Cunrath et al. 2015). It has been modified to align with our specific requirements and experimental constraints. These adaptations include accommodating a substantial bacterial quantity and excluding superfluous steps that might introduce bias. The 40 mL suspension of *P. aeruginosa* at $OD_{600nm}=0.5$ was incubated with various calcium solutions in 50 mL Falcon™ tubes for 2 h at 30 °C. After this incubation, the supernatants were obtained through centrifugation (9871×*g* for 5 min). The bacterial pellets were treated as follows:

(a) Re-suspended in 1 mL of a mixture containing 200 mM Tris (tris(hydroxymethyl)aminomethane, used as a buffer solution), 1 mM EDTA, and 20% sucrose (referred to hereafter as Tris–EDTA-sucrose) containing wo a final concentration of 200 µg/mL of lysozyme) were added to

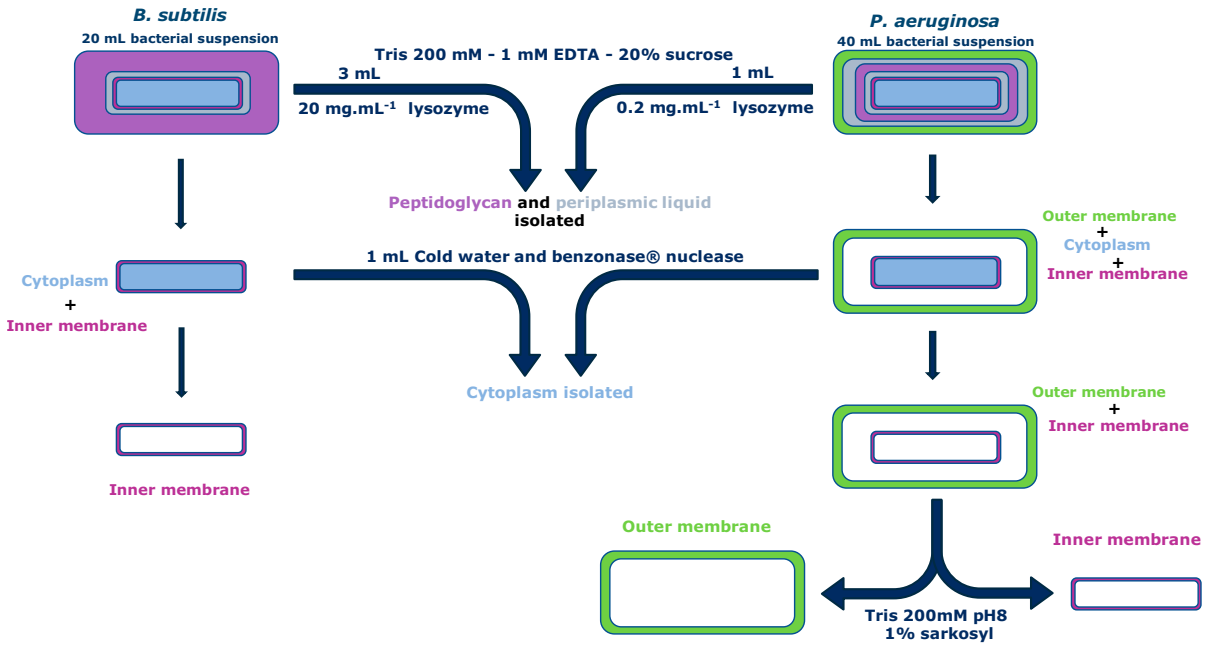

Fig. 1 Simplified schematic of the cellular fractionation protocol for *B. subtilis* and *P. aeruginosa*. Indication of different solutions used for each separation step are provided

this mixture. The solution was vortexed and then incubated on ice for 1 h. After the incubation, the tubes were centrifuged (6134×*g* for 10 min at 4 °C). The resulting supernatant contained the periplasmic liquid and peptidoglycan, while the pellets represented the spheroplasts (denoting *P. aeruginosa* cells devoid of the outer membrane). The pellets underwent three washes with 500 µl of Tris–EDTA-sucrose.

(b) Re-suspended in 1 ml of 4 °C water, the pellets were vortexed and homogenized through successive aspirations. Following this, 1 µl of benzonase® nuclease (used to degrade DNA and RNA, Sigma) was introduced to each sample. After another round of vortexing, the samples were incubated (220 rpm for 1 h at 37 °C). Post-incubation, the solution was transferred to microtubes and subjected to ultracentrifugation (71,577×*g* for 40 min at 4 °C). The resulting supernatants were indicative of the cytoplasm. The pellets underwent three washes with 500 µl of freshly prepared 4 °C filter-sterilized pure water.

(c) Re-suspended in 1 ml of a solution comprising 200 mM Tris at pH 8 and 1% sarkosyl (used for cell lysis and membrane solubilization). This resuspension was achieved through successive aspirations to disrupt the pellets, followed by vortexing. The mixture was shaken on a rotary shaker for 1 h. The samples were then centrifuged (71,577×*g* for 40 min at 4 °C). The resulting supernatants indicated the presence of the inner membrane, whereas the pellets represented the outer membrane. The pellets were washed thrice with 500 µl of 4 °C filter-sterilized pure water. At each stage, the washing waters were collected for concentration analysis, facilitating the proper allocation of waste to their corresponding cellular compartments.

Bacillus subtilis

The composition of cell walls in *B. subtilis* and *P. aeruginosa* differs due to their classification as Gram-positive and Gram-negative bacteria, respectively. Consequently, it was necessary to adapt the cell fractionation protocol. Initial attempts at cell fractionation for *B. subtilis*, using the same experimental conditions as those for *P. aeruginosa*, revealed an absence of protoplast transformation following lysozyme

treatment. Several approaches were explored to address this by various factors such as contact time, bacterial concentration, and lysozyme concentration. Ultimately, a significant increase in lysozyme concentration and a reduction in bacterial number per tube led to successful peptidoglycan digestion within a 1 h contact period. This transition of bacteria into protoplasts was confirmed through microscopic examination before progressing with the experiment.

The *B. subtilis* cell fractionation protocol was executed according to the subsequent description. Following a bacterial incubation phase with the calcium solution in 50 ml Falcon™ centrifuge tubes (at 220 rpm for 2 h and 30 °C), the resulting mixture underwent centrifugation (9871×*g* for 5 min). Subsequently, supernatants were collected, while the bacterial pellets were subjected to the following steps: Then: (a) The pellets were re-suspended in 3 ml of a Tris–EDTA-sucrose mixture containing 20 mg/ml of lysozyme. After vortexing, the mixture was incubated on ice for 1 h.

Following the incubation, the tubes underwent centrifugation (6134×*g* for 10 min at 4 °C). The resulting supernatants contained peptidoglycan, while the pellets represented protoplasts. The pellets were subjected to three washes, each involving 500 µl of Tris–EDTA-sucrose.

(a) The protoplasts were re-suspended in 1 ml of cold water (4 °C), followed by vortexing and homogenization via successive pipetting. Then, 1 µl of benzonase® nuclease was introduced to the samples, which were again vortexed before incubation (220 rpm for 1 h at 37 °C). Post-incubation, the protoplasts from step (b) were transferred to microtubes and subjected to centrifugation (71,577×*g* for 40 min at 4 °C). The resulting supernatants corresponded to the cytoplasm, while the pellets contained the cytoplasmic membrane.

Analytical procedures

To assess calcium concentration in the supernatants and bacterial digests, a portion of each sample was diluted with 0.25 N HNO_3 and subjected to analysis using an ICP-AES (iCAP 6000 series, ThermoFisher Scientific™). This instrument exhibited an accuracy nearing 3% for calcium measurements, which was verified over the entire calibration interval.

Calcium isotopic measurements were conducted on a mixture of each adsorption replicate for a given experiment. They were measured on a TIMS (ThermoFisher Scientific Triton™) following the laboratory protocol (Schmitt et al. 2009, 2017; Brazier et al. 2019; 2020). The samples were prepared by adding 0.14 µmol of Ca to 0.01 µmol of a ^{42}Ca–^{43}Ca double spike (i.e., $^{42}Ca/^{43}Ca$ spike ratio of 5, following Holmden (2005)) and dried down at 70 °C on a hotplate. Then, all samples and internal standard (Atlantic seawater, Schmitt et al. 2001; Hippler et al. 2003) solutions were loaded into ion-exchange chromatographic columns (high-density polyethene) filled with 2 ml of DGA normal resin (TODGA) from Triskem™ (Horwitz et al. 2005; Romaniello et al. 2015). The purified samples were collected in 0.1 N HCl in Savillex™ beakers, with an addition of 0.2 ml of distilled HNO_3 and suprapure H_2O_2 before being heated and dried down at 70 °C and then converted into nitric form by dissolution in 0.5 ml of 2 N HNO_3 and dried down one last time. After this, the samples were dissolved in 1.5–3 µl 1 N HNO_3 and loaded on previously outgassed and under primary vacuum oxidized tantalum single filaments (99.995% purity). Note that the total Ca blank for this separation represents less than a 0.2% contribution to the Ca from samples and can be neglected.

Measured values of the isotopic analysis were expressed as $\delta^{44/40}Ca$ in per mil relative to the NIST SRM915a standard (Hippler et al. 2003; Eisenhauer et al. 2004), using the following formula:

$$\delta^{44/40}Ca = \left(\frac{^{44}Ca/^{40}Ca_{sample}}{^{44}Ca/^{40}Ca_{SRM915a}} - 1 \right) \times 1000 \quad (1)$$

To directly assess the apparent isotopic fractionation, our results will be expressed as a difference ($\Delta^{44/40}Ca_i$) between the measured Ca isotopic composition in the final aqueous or solid phase ($\delta^{44/40}Ca_i$) and that of the initial solution ($\delta^{44/40}Ca_{ini}$):

$$\Delta_{\delta^{44}/^{40}Ca_i} = \delta^{44}/^{40}Ca_i - \delta^{44}/^{40}Ca_{IS} \quad (2)$$

where "i" represents LAA or BAA.

The associated propagated uncertainty (Δ_{error}, in ‰) can be expressed as

$$\Delta_{error\,(\Delta^{44}/^{40}Ca_i)} = \sqrt{\left(\Delta_{\delta 44/^{40}Ca_i}\right)^2 + \left(\Delta_{\delta 44/^{40}Ca_{IS}}\right)^2} \quad (3)$$

The average internal repeatability achieved throughout the study was 0.07‰, determined from repeated measurements of NIST SRM 915a (2SD, N = 124). Likewise, repeated measurements of the initial calcium solution yielded a value of 0.89 ± 0.11‰ (2SD, N = 6). The external uncertainty, as calculated from external long-term sample replicates, amounted to 0.10‰ (2SD, N = 14) for $\delta^{44/40}$Ca values. Using these figures and Eq. (3), the propagated error associated with $\Delta^{44/40}$Ca was determined to be 0.15‰. To gauge the accuracy of our measurements, we employed an in-house Atlantic seawater standard (1.88‰ ± 0.11, 2SD, N = 38) during the same timeframe. The obtained values and references aligned with those reported by Hippler et al. (2003) and Heuser et al. (2016).

Results

Adsorption experiments on vegetative bacteria

Variation of Ca concentration of the initial solution

We observed a linear relationship between the residual calcium concentration in the supernatant and the initial calcium concentration in solution for both *B. subtilis* and *P. aeruginosa* ($R^2 > 0.99$) (Fig. 2a). However, a slight difference emerged between the two bacteria. *Pseudomonas aeruginosa* exhibited a more rapid saturation with calcium as the concentration increased. Specifically, at 5.0 µg/ml, *P. aeruginosa* retained 61 ± 2% of the initial calcium concentration in the supernatant, whereas *B. subtilis* retained around 79 ± 3% (equivalent to approximately 40% and 20% of adsorbed calcium for *P. aeruginosa* and *B. subtilis*, respectively). Conversely, the disparity was less noticeable at lower concentrations (around 20%) (Table 1).

Experiments varying $[Ca^{2+}]_{IS}$ were conducted at pH 5.6 with a 2 h interaction duration. Experiments varying interaction time were conducted at pH 5.6 and $[Ca^{2+}]_{IS}$ equal to1.6 µg/ml. Experiments varying initial pH were conducted at $[Ca^{2+}]_{IS}$ equal to 1.6 µg/ml at pH 5.6, and $[Ca^{2+}]_{IS}$ equal to 1.5 µg/ml at pHs 5 and 7, with a 2 h interaction duration.

LAA refers to the liquid after adsorption, while BAA refers to the bacteria after adsorption. IS refers to initial solution.

Results obtained with dead bacteria (at 0.5 µg/ml) indicated discrepancies in sorption compared to alive counterparts, particularly for *P. aeruginosa*: residual calcium remained in the solution after adsorption with dead bacteria (21 ± 2%), whereas with alive bacteria (at 0.5 µg/ml), almost all the calcium in the solution was sequestered within the bacterial cells (3 ± 1% Ca remaining in solution). In contrast, for *B. subtilis*, no significant difference was discernible between living and dead bacteria, and no Ca remained in solution (Table 1).

No discernible isotopic fractionation is evident in the liquid following adsorption/incorporation, irrespective of the varying conditions (such as the percentage of residual calcium in the supernatant or the state of bacteria being dead or alive). This holds even when the residual calcium in the supernatant is below 10%, which suggests that calcium availability is limited ($\delta^{44/40}Ca_{LAA} = 0.86 \pm 0.11$‰ (2SD, N = 4) and 0.84 ± 0.11‰ (2SD, N = 3) for *B. subtilis* and *P. aeruginosa*, respectively and $\delta^{44/40}Ca_{BAA} = 0.85 \pm 0.06$ ‰ (2SD, N = 6) and 0.81 ± 0.13‰ (2SD, N = 4) for *B. subtilis* and *P aeruginosa*, respectively, while $\delta^{44/40}Ca_{IS} = 0.89 \pm 0.11$‰ (2SD, N = 6)) (Table 1 and paragraph 2.5). From these results, the concentration of the calcium solution was established at 1.55 ± 0.14 µg/ml (2SD, N = 2) for the kinetic and pH experiments. These experimental parameters were selected to obtain an optimal balance between calcium adsorption and residual calcium in solution to facilitate isotopic analysis.

Kinetics

The kinetic study depicted in Fig. 2c was conducted at pH 5.6, between 0 and 250 min, and our findings revealed an immediate occurrence of adsorption/incorporation for both bacterial strains, in similar average proportions (20 ± 14%, N = 6, 2 SD, residual calcium in solution for *P. aeruginosa* compared to 23 ± 5%, N = 6, 2 SD, for *B. subtilis*). We can notice that residual calcium slightly increased during the first half-an-hour of contact for *B. subtilis* (resulting in 14 ± 7%, N = 3, 2 SD residual calcium in the supernatant from 5 to 35 min, and then 26 ± 2% from 65 to 245 min, N = 3, 2 SD). Between the 1 and 4 h

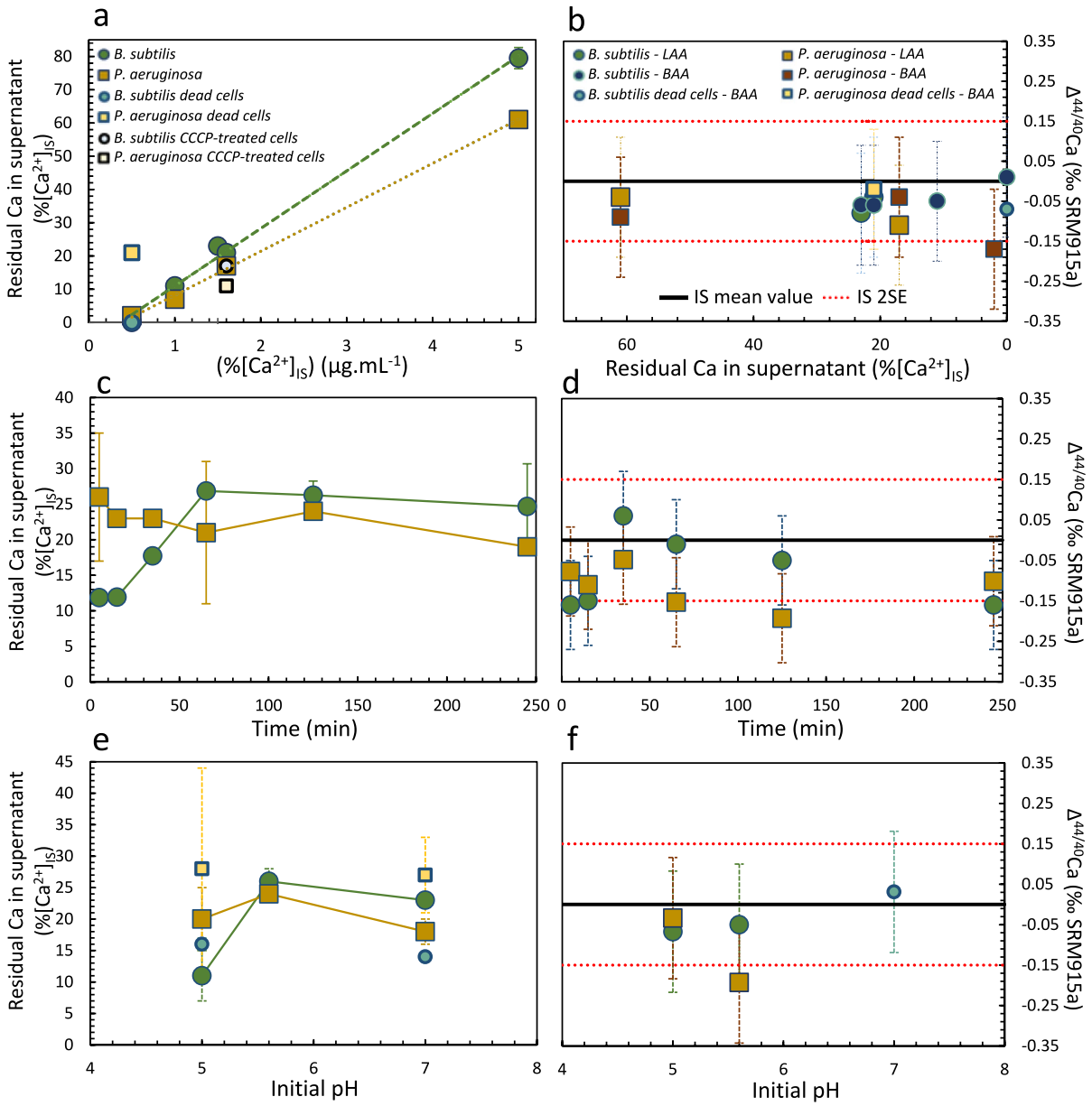

Fig. 2 Elemental and isotopic measurements of Ca adsorption experiments on vegetative bacteria: **a** Residual Ca in the supernatant, expressed as a percentage of the initial Ca in the solution, as a function of the initial solution concentration, and **b** corresponding $\Delta^{44/40}$Ca values; **c** Residual Ca in the supernatant, expressed as a percentage of the initial Ca in the solution, as a function of the interaction time, and **d** corresponding $\Delta^{44/40}$Ca values; **e** Residual Ca in the supernatant, expressed as a percentage of the initial Ca in the solution, as a function of the initial pH of the solution, and **f** corresponding $\Delta^{44/40}$Ca values

interval, the trend appeared stable for both bacteria (Fig. 2c). Notably, from an isotopic perspective, the recorded values fell within the range of analytical reproducibility (Fig. 2d).

Table 1 Amount of residual Ca in the supernatant and Ca apparent isotopic fractionation between the initial solution and the supernatant or the bacteria measured after adsorption experiments in various conditions

Sample	pH	$[Ca]_{IS}$	State of bacteria	OD600nm	N	Time	$[Ca^{2+}]$ in supernatant				$\delta^{44/40}Ca_{LAA}$	$\delta^{44/40}Ca_{BAA}$	$\Delta^{44/40}Ca_{LAA}$	$\Delta^{44/40}Ca_{BAA}$
		µg/ml				min	µg/ml	2SD	%	2SD	‰			
B. subtilis														
Conc. var	5.6	0.5	Dead	0.5	2	125	0.00	0.02	0	1		0.82		− 0.07
	5.6	0.5	Alive	0.5	4	125	0.00	0.02	0	1		0.90		0.01
	5.6	1.0	Alive	0.5	2	125	0.09	0.09	11	2		0.84		− 0.05
	5.6	1.5	Alive	0.5	2	125	0.35	0.03	23	2	0.81	0.83	− 0.08	− 0.06
	5.6	1.6	Alive	0.5	2	125	0.45	0.30	28	1	0.85	0.83	− 0.04	− 0.06
	5.6	1.6	Alive	1.0	3	125	0.08	0.02	5	1	0.94		0.05	
	5.6	5.0	Alive	0.5	2	125	3.97	0.19	79	3	0.86	0.86	− 0.03	− 0.03
Kinetics	5.6	1.6	Alive	0.5	2	5	0.19	0.02	12	1	0.73		− 0.16	
	5.6	1.6	Alive	0.5	2	15	0.19	0.02	12	1	0.74		− 0.15	
	5.6	1.6	Alive	0.5	2	35	0.29	0.03	18	1	0.95		0.06	
	5.6	1.6	Alive	0.5	2	65	0.43	0.04	27	1	0.88		− 0.01	
	5.6	1.6	Alive	0.5	2	125	0.42	0.03	26	2	0.84		− 0.05	
	5.6	1.6	Alive	0.5	2	245	0.40	0.10	25	6	0.73		− 0.16	
pH	5.0	1.5	Alive	0.5	2	125	0.17	0.06	11	4	0.82		− 0.07	
	5.0	1.5	Dead	0.5	2	125	0.24	0.02	16	1				
	7.0	1.6	Alive	0.5	2	125	0.37	0.02	23	1				
	7.0	1.6	Dead	0.5	2	125	0.22	0.02	14	1	0.92		0.03	
CCCP	5.6	1.6	Alive	0.5	2	125	0.27	0.11	17	7				
P. aeruginosa														
Conc. var	5.6	0.5	Dead	0.5	2	125	0.11	0.04	21	2		0.87		− 0.02
	5.6	0.5	Alive	0.5	2	125	0.01	0.01	3	1		0.72		− 0.17
	5.6	1.0	Alive	0.5	2	125	0.07	0.07	7	1				
	5.6	1.6	Alive	0.5	2	125	0.27	0.02	17	1	0.78	0.85	− 0.11	− 0.04
	5.6	1.6	Alive	1.0	3	125	0.06	0.03	4	2	0.88		− 0.01	
	5.6	5.0	Alive	0.5	4	125	3.05	0.04	61	2	0.85	0.80	− 0.04	− 0.09
Kinetics	5.6	1.6	Alive	0.5	2	5	0.42	0.14	26	9	0.81		− 0.08	
	5.6	1.6	Alive	0.5	2	15	0.37	0.04	23	1	0.78		− 0.11	
	5.6	1.6	Alive	0.5	2	35	0.37	0.04	23	1	0.84		− 0.05	
	5.6	1.6	Alive	0.5	2	65	0.34	0.16	21	10	0.74		− 0.15	

Table 1 (continued)

Sample	pH	$[Ca]_{IS}$	State of bacteria	OD600nm	N	Time	$[Ca^{2+}]$ in supernatant				$\delta^{44/40}Ca_{LAA}$	$\delta^{44/40}Ca_{BAA}$	$\Delta^{44/40}Ca_{LAA}$	$\Delta^{44/40}Ca_{BAA}$
		µg/ml				min	µg/ml	2SD	%	2SD	‰			
	5.6	1.6	Alive	0.5	2	125	0.38	0.04	24	1	0.70		− 0.19	
	5.6	1.6	Alive	0.5	2	245	0.30	0.03	19	1	0.79		− 0.10	
pH	5.0	1.5	Alive	0.5	2	125	0.30	0.08	20	5	0.86		− 0.03	
	5.0	1.5	Dead	0.5	2	125	0.42	0.24	28	16				
	7.0	1.6	Alive	0.5	2	125	0.29	0.03	18	2				
	7.0	1.6	Dead	0.5	2	125	0.43	0.10	27	6				
CCCP	5.6	1.6	Alive	0.5	2	125	0.18	0.02	11	1	0.93		0.04	

The concentrations were measured in each replicate, and the average is presented here. The different replicates were pooled to perform the isotopic measurements. The percentage corresponds to the percentage of initial Ca remaining in solution, and the following 2SD represents the 2SD of the % measurement

LAA liquid after adsorption, *BAA* bacteria after adsorption, *IS* initial solution

Effect of the transfer processes inhibition

To assess the degree of active calcium incorporation in bacteria during our experiments, bacterial cells were treated with the proton-motive force inhibitor CCCP. Figure 2a portrays the residual calcium in the supernatant of both bacterial strains under various physiological conditions: alive, dead, or in the presence of CCCP. In the case of *P. aeruginosa*, residual calcium in the supernatant amounted to $11 \pm 1\%$ of the initial calcium concentration when CCCP was present, in contrast to $17 \pm 1\%$ under the same conditions but without CCCP. Similarly, for *B. subtilis*, residual calcium in the supernatant is equal to $17 \pm 7\%$ of the initial calcium concentration with CCCP, compared to $21 \pm 1\%$ without its usage (Table 1). Both *P. aeruginosa* and *B. subtilis* exhibited a reduction in residual calcium in the supernatant, leading to an increase in adsorption (a respective increment of + 13% and + 14%). Importantly, these experiments yielded no observable isotopic fractionation (Fig. 2b).

pH variation

Following a 2 h interaction between the calcium solution and bacteria at OD_{600} equal to 0.5, 1.5 or 1.6 µg/l Ca, at pH 5, 5.6 or 7, there are differences in the percentages of Ca remaining in the solution between live and dead bacteria and between bacteria. For *B. subtilis*, for dead bacteria, there are few differences between pH 5 and 7 ($16 \pm 1\%$ and $14 \pm 1\%$ of residual Ca, respectively), whereas for live bacteria, the percentage varies more ($11 \pm 4\%$ and $23 \pm 1\%$ of Ca residual, respectively. For *P. aeruginosa*, there are few differences based on pH, whether the bacteria are dead (28 ± 16 and 27 ± 6, at pH 5 and 7 respectively) or alive (20 ± 5 and 18 ± 2, at pH 5, and 7 respectively). At pH 5.6, the percentage of Ca in the residual liquid is similar (27 ± 3, N = 2, 2SD and $21 \pm 10\%$, N = 2, 2 SD, for *B. subtilis* and *P. aeruginosa*, respectively). For an OD_{600nm} equal to 1, we observe less Ca in solution (5 ± 1 and $4 \pm 2\%$ for *B. subtilis* and *P. aeruginosa*, respectively), (Table 1). No substantial isotopic fractionation was observed; the values fell within the range of error bars (Fig. 2f).

Note also that over the pH range considered in this study, Ca is either in dissolved or adsorbed form and is never located in precipitated forms. Calculations

performed with VisualMinteq TM version 3.1 software associated with the "thermo.vdb" thermodynamic database (Gustafsson 2013) showed that all solutions recovered after adsorption and desorption experiments are strongly undersaturated with respect to Ca $(NO_3)_2$, $CaCO_3$, and $Ca_2P_2O_7$ solid phases. Thus, isotopic fractionation due to Ca precipitation in solution can be excluded.

Cell fractionation experiments for vegetative bacteria

Pseudomonas aeruginosa

Pseudomonas aeruginosa cell fractionation was conducted using two distinct calcium (Ca) concentrations, representing conditions with limited and non-limiting Ca availability. As a result, two different total Ca amounts were present in the cell fractions: 87 µg Ca in experiment n°1 and 200 µg in experiment n°2. Calcium was primarily sequestered within bacterial wall compartments, albeit in varying proportions contingent upon the initial total Ca content (Table 2).

In the first experiment, Ca was predominantly localized in the peptidoglycan and periplasmic space (55 ± 6%) and the outer membrane (18 ± 7%) (Table 2). Lesser quantities of Ca were found within the cytoplasm (16 ± 10%) and the inner membrane (11 ± 17%). Conversely, the second experiment exhibited an increased allocation of Ca within the peptidoglycan + periplasmic fraction (64 ± 6%) (Table 2). Within this context, the Ca content of the outer membrane constituted 17 ± 2% of the overall Ca content, while the cytoplasm and inner membrane contained 10 ± 6% and 9 ± 14% of the total Ca, respectively. Notably, no isotopic fractionation was discernible within any of the cellular compartments.

Bacillus subtilis

Owing to the smaller quantity of bacteria employed in the *B. subtilis* experiments, the detected Ca levels within the samples were comparatively reduced compared to those observed in *P. aeruginosa* ("*Pseudomonas aeruginosa*" section). In the first experiment, 48 µg Ca was measured, while the second experiment recorded 105 µg of Ca.

In a manner akin to *P. aeruginosa*, Ca was predominantly sequestered within the cell wall of *B. subtilis*,

Table 2 Amount of Ca present in the different cell-compartments of *B. subtilis* and *P. aeruginosa*, and Ca apparent isotopic fractionation between the initial solution and the cell-compartments measured after adsorption experiments at pH 5.6 and in two different conditions of total Ca amount for each bacterium

The concentrations were measured in each replicate, and the average is presented here. The different replicates were pooled to perform the isotopic measurements. The percentage corresponds to the percentage of initial Ca remaining in solution, and the following 2SD represents the 2SD of the % measurement

BAA bacteria after adsorption

Sample	N	$Ca_{average}$				$\Delta^{44/40}Ca_{BAA}$
		µg	2SD	%	2SD	‰
P. aeruginosa						
Exp. 1: 87 µg Ca						
Peptidoglycan and periplasm	3	15.85	1.59	55	6	− 0.01
Cytoplasm	3	4.67	2.8	16	10	0.04
Inner membrane	3	3.3	4.95	11	17	0.03
Outer membrane	3	5.09	2.04	18	7	− 0.07
Exp. 2: 200 µg Ca						
Peptidoglycan and periplasm		42.87	4.29	64	6	− 0.03
Cytoplasm	3	6.49	3.89	10	6	0.01
Inner membrane	3	6.08	9.12	9	14	0.04
Outer membrane	3	11.36	1.14	17	2	− 0.02
B. subtilis						
Exp. 1: 48 µg Ca						
Peptidoglycan and periplasm	3	13.59	1.65	85	10	0.03
Cytoplasm	3	0.7	0.42	4	2	–
Inner membrane	3	1.79	2.67	11	16	–
Exp. 1: 105 µg Ca						
Peptidoglycan and periplasm	3	32.53	5.73	93	16	0.02
Cytoplasm	3	0.88	0.51	3	2	–
Inner membrane	3	1.56	3.17	4	8	–

which, in this case, corresponded exclusively to peptidoglycan. In the first experiment, this encompassed 85 ± 10% of the total Ca content, with the remaining portion being apportioned between the outer membrane (11 ± 16%) and the cytoplasm (4 ± 2%). During the second experiment, the prevalence of Ca within peptidoglycan was even more pronounced (93 ± 16%), while the inner membrane (4 ± 8%) and cytoplasm (3 ± 2%) exhibited diminished proportions of Ca. Notably, isotopic measurements of peptidoglycan (the sole fraction amenable to measurement due to the scant Ca content in the other fractions) exhibited no discernible isotopic fractionation.

Experiments on sporulated bacteria

Control spore pellets, devoid of exposure to the Ca solution, were generated at OD_{600nm} values of 0.5 and 1.5. These control samples were employed to ascertain the initial presence of Ca within the spores before the adsorption experiments, yielding Ca concentrations of 0.57 µg/ml within the spore suspension at $OD_{600nm} = 0.5$ and 1.58 µg/ml at $OD_{600} = 1.5$, respectively. Thus, contrary to vegetative bacteria, the control spore samples contain Ca. They are also enriched in ^{40}Ca compared to the sporulation medium ($\Delta^{44/40}Ca$ sporulation medium = 0.18‰) in which they were cultured (Table 3). It is also observed that the intensity of fractionation in the spores is higher at $OD_{600} = 0.5$ ($\Delta^{44/40}Ca_{spores-IS} = -1.02 \pm 0.15$‰) compared to $OD_{600} = 1.5$ ($\Delta^{44/40}Ca_{spores-IS} = -0.40 \pm 0.15$‰) (Table 3), with a total fractionation amplitude of 1.20‰ and 0.58‰, respectively, between the spores and the sporulated medium.

Once sporulated, the spore pellets were placed in contact with a Ca solution. Figure 3a illustrates the residual Ca content present in the supernatant following exposure to *B. subtilis* spore suspensions. Notably, the spores demonstrated a diminished capacity for Ca uptake from the solution compared to their vegetative bacterial counterparts. The extracted Ca content ranged from 10% (resulting in 90 ± 3% residual Ca within the supernatant at $OD_{600nm} = 0.5$) to 86% (leaving 14 ± 1% residual Ca within the supernatant at $OD_{600nm} = 4.5$), diverging from the range of 79–83% observed for vegetative bacteria. Intriguingly, the quantity of Ca extracted from the solution exhibited a linear increase across the range from $OD_{600nm} = 0.5$ to $OD_{600nm} = 4.5$, progressing

Table 3 Amount of residual Ca in the supernatant and Ca apparent isotopic fractionation between the initial solution and the supernatant or the spores measured after adsorption experiments in various OD_{600nm} conditions

Sample	pH	$[Ca^{2+}]_{IS}$	State of bacteria	OD600nm	N	Time	$[Ca^{2+}]$ in supernatant				$\delta^{44/40}Ca_{sporulated\ medium}$	$\delta^{44/40}Ca_{LAA}$	$\delta^{44/40}Ca_{BAA}$	$\Delta^{44/40}Ca_{sporulated\ medium}$	$\Delta^{44/40}Ca_{LAA}$	$\Delta^{44/40}Ca_{BAA}$
		µg/ml				min	µg/ml	2SD	%	2SD	‰					
	5.6	1.6	Spores	0.5	3	120	1.44	0.05	90	3	–	0.76	0.08	–	− 0.13	− 0.81
	5.6	1.6	Spores	1	3	120	1.3	0.08	81	5	–	–	–	–	–	–
	5.6	1.6	Spores	1.5	3	120	0.94	0.03	59	2	–	0.78	0.63	–	− 0.11	− 0.26
	5.6	1.6	Spores	2.5	3	120	0.77	0.03	48	2	–	–	–	–	–	–
	5.6	1.6	Spores	3.5	2	120	0.26	0.08	16	5	–	0.75	0.45	–	− 0.14	− 0.44
	5.6	1.6	Spores	4.5	2	120	0.22	0.02	14	1	–	0.85	0.63	–	− 0.04	− 0.26
Sporurated medium	–	–	–	–	–	–	–	–	–	–	1.07	–	–	0.18	–	–
Control sample	–	–	Spores	0.5	3	–	–	–	–	–	–	–	− 0.13	–	–	− 1.02
Control sample	–	–	Spores	1.5	3	–	–	–	–	–	–	–	0.49	–	–	− 0.40

The concentrations were measured in each replicate, and the average is presented here. The different replicates were pooled to perform the isotopic measurements

LAA liquid after adsorption, *BAA* bacteria after adsorption, *IS* initial solution

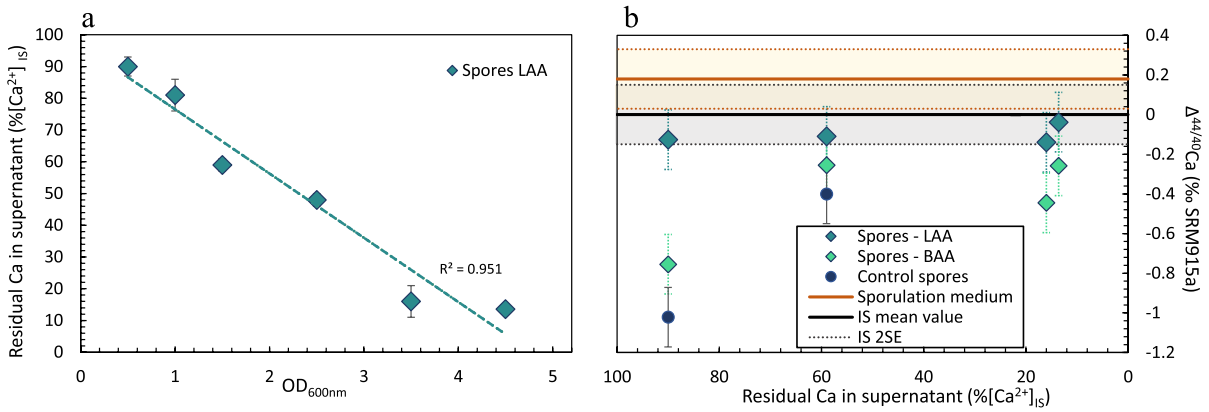

Fig. 3 Elemental and isotopic measurements of Ca adsorption experiments on *B. subtilis* spores. **a** The residual Ca in the supernatant, expressed as a percentage of the initial Ca in the solution, as a function of the OD_{600nm} of the bacterial suspension. Experiments were conducted at pH 5.6 with a 2 h interaction duration, and $[Ca^{2+}]_{IS}$ equal to 1.6 µg/ml. **b** The values of $\Delta^{44/40}Ca$ as a function of the percentage of residual calcium in the supernatant. The values of spore controls (spore pellets without Ca adsorption) and the sporulation medium used for spore culture are also presented. LAA liquid after adsorption, BAA bacteria after adsorption, IS initial solution

from 10 to 86% (correlation coefficient $R^2=0.951$, N=6) (Table 3).

In addition to the initial calcium isotope fractionation during sporulation, we have also observed a subsequent phenomenon wherein the spore pellets experience an enrichment in the isotope ^{44}Ca after sorption of calcium from the solution, compared to their initial values ($\Delta^{44/40}Ca$ equal to 0.21‰ for $OD_{600nm}=0.5$ and 0.14‰ for $OD_{600nm}=1.5$, see Table 3 and Fig. 3b). We exclusively conducted spore control measurements at OD_{600} values of 0.5 and 1.5. Nevertheless, the isotopic profiles of bacteria post-adsorption exhibit similarities within the range of analytical errors for OD_{600nm} values of 1.5, 3.5, and 4.5 (-0.27 ± 0.22, with a 2-standard deviation range, N=3). Thus, we assume that spore control values remain consistent across OD_{600nm} values of 1.5, 3.5, and 4.5. Interestingly, in parallel, the supernatants following the adsorption process do not exhibit any fractionation ($\Delta^{44/40}Ca$ is equal to -0.11 ± 0.09‰, N=4, 2SD) despite up to 86% of the calcium being adsorbed (Fig. 3b).

Discussion

Absence of fractionation during the adsorption/incorporation of Ca onto/in vegetative bacteria

Regarding elemental adsorption/incorporation, various parameters, such as pH, calcium concentration, and incubation time, showed an evident influence on the quantity of adsorbed calcium. Distinct discrepancies were observed between *B. subtilis* and *P. aeruginosa*. pH appeared to exert a more pronounced influence on *B. subtilis*, displaying enhanced adsorption/incorporation at a pH of 5. In contrast, for *P. aeruginosa*, variations were less significant across different pH values. Similarly, the quantity of adsorbed/incorporated calcium exhibited temporal variations for both bacterial strains, albeit in distinct manners.

Initially, *B. subtilis* exhibited higher calcium uptake, which was subsequently released within 2 h. Consequently, *P. aeruginosa* displayed a slightly higher adsorbed/incorporated calcium level. Notably,

the kinetics revealed a marginal increase in adsorbed/incorporated calcium for both bacterial strains after 4 h. Nevertheless, caution is advised when extrapolating this trend to ascertain a longer-term equilibrium due to the limitations in conducting extended adsorption experiments with these bacteria.

In contrast, the process of adsorption/incorporation did not exhibit any discernible isotopic fractionation, regardless of the prevailing conditions for either *P. aeruginosa* or *B. subtilis*. Limited knowledge of elemental fractionation associated with the adsorption/incorporation onto/in bacteria is available. Nonetheless, investigations related to the adsorption or incorporation of metal ions, such as Zn, Cu, Mo, Fe, or Cr, have been carried out (Wasylenki et al. 2007; Navarette et al. 2011; Kafantaris and Borrock 2014; Mullholand et al. 2015; Zhang et al. 2018), revealing noticeable isotopic fractionations. These diverse studies have demonstrated that isotopic fractionation of an element in contact with bacteria can be attributed to their complexation with functional groups on the bacteria's surface or active mechanisms that necessitate energy.

Through experiments conducted on both live and dead bacteria, specifically *Pseudomonas fluorescens* LB 300 and *Shewanella oneidensis* MR 1, to assess the impact of metabolic activity, Zhang et al. (2018) deduced that the reduction of Cr(VI) to Cr(III) primarily results from metabolic activity. In contrast, investigations involving *Azotobacter vinelandii* (Wasylenki et al. 2007) suggested that while Mo undergoes kinetic fractionation during assimilation, complexation with ligands might also partially induce this fractionation. Moreover, concerning Fe, which does not exhibit a kinetic effect, indications point toward fractionation occurring through complexation processes (Wasylenki et al. 2007).

Given the range of methodologies and variables used across these diverse studies and the discrepancies in outcomes for various elements, establishing direct parallels with our findings seems challenging. However, in contrast to the studies above, the absence of isotopic fractionation in our research implies the adsorption/incorporation of ^{40}Ca and ^{44}Ca in equivalent proportions. The disparity in the impact of various parameters on the interaction between bacteria and calcium can be elucidated by the distinct nature of the cell walls in *B. subtilis* and *P. aeruginosa*.

Distribution of calcium in bacteria and highlighting the proportions of adsorbed and incorporated Ca

To elucidate the absence of isotopic fractionation in our experimental findings, it becomes imperative to precisely ascertain the fate of calcium during our experiments. This entails determining the precise ratios at which calcium becomes adsorbed and/or incorporated by the bacteria while identifying the potential mechanisms at play. Previous data establishes that calcium is pivotal in various bacterial processes, including maintaining cell structure, cell division, and sporulation (Smith 1995). Furthermore, it has been demonstrated that bacteria exercise precise control over their calcium content, typically within the range of 100–300 nM (Gangola and Rosen 1987; Knight et al. 1991; Futsaether and Johnsson 1994; Herbaud et al. 1998; Jones et al. 1999; Torrecilla et al. 2000). Bacteria also employ various regulatory mechanisms, encompassing primary and secondary transporters and calcium-binding proteins, to maintain calcium homeostasis (Norris et al. 1996; Paulsen et al. 2000; Waditee et al. 2004). These intricate systems further underline the need to unravel the precise interactions and dynamics governing calcium within the context of our experiments.

To explore the impact of metabolic activity on calcium uptake by bacteria, experiments were undertaken to assess the influence of bacterial physiological state—whether the cells were viable or dead—on the quantity of calcium extracted from the solution (Table 1). In the context of *P. aeruginosa*, disparities in adsorption/incorporation between live and deceased bacteria could suggest that viable cells integrate a noteworthy portion of calcium (approximately 8–9% of the calcium extracted from the solution). Conversely, when examining *B. subtilis*, the observation that deceased bacteria exhibit the highest levels of adsorption/incorporation at pH 7 appears to challenge this hypothesis. Consequently, it is plausible that the observed distinctions are partly attributed to the bacterial incorporation of calcium. However, these variations might also be partially attributed to chemical factors arising from alterations in the bacterial surface, leading to modified interactions with calcium. As such, it is essential to recognize that conducting experiments solely comparing live and dead bacteria falls short of comprehensively estimating the

fraction of calcium potentially incorporated via bacterial metabolic activity.

An alternative approach to address this inquiry involves employing CCCP to hinder the protonmotive force and impede calcium incorporation at the membrane level. Nevertheless, in the context of our experiments, the utilization of CCCP yielded an unexpected outcome—an increase in the quantity of calcium extracted from the solution (a rise of + 13% for *P. aeruginosa* and + 14% for *B. subtilis*, Table 1). Contrary to our observations, a decrease in incorporation could have potentially signalled a reduction in the overall amount of calcium extracted from the solution by the bacteria.

After these findings, the cellular fractionation experiments ultimately answered this inquiry. Our investigations revealed that calcium primarily accumulates within wall compartments and that its intracellular integration—spanning the cytoplasm and internal membranes—constitutes a minority fraction. Remarkably, the Gram-negative bacteria's surface adsorbs less than 20% of calcium taken from the solution, chiefly on the outer membrane. This outer membrane possesses carboxyl groups recognized for inducing plant calcium isotopic fractionation (Cobert et al. 2011b; Schmitt et al. 2013). Notably, most calcium transverses the outer membrane, adhering to the peptidoglycan layer. For *B. subtilis*, the preponderance of calcium is adsorbed onto the peptidoglycan matrix.

Our exploration shows that no detectable isotopic fractionation exists, irrespective of the cellular compartment under consideration (Table 2), even within the outer membrane housing carboxyl groups—a context in which fractionation might have been anticipated. This circumstance might suggest that calcium experiences passive integration within bacterial cells, void of any marked fractionation—a notion akin to the supposition surrounding calcium entry into roots (Cobert et al. 2011b). This conclusion is corroborated by the study of Braud et al (2009), which demonstrates that the uptake of Ca in *P. aeruginosa* occurs through diffusion across the membrane via porins or bound at the cell surfaces.

Isotopic fractionation during sporulation

The difference in fractionation in control spore pellets was not expected since the adjustment of OD_{600} involves dilution, which is not supposed to impact isotopic proportions. It is possible that the spores, which have been stored in several centrifuge tubes, exhibit heterogeneity in the isotopic proportions of Ca they contain. This heterogeneity could be because not all bacteria sporulate simultaneously but gradually, implying that the isotopic proportions of Ca in the sporulation medium can vary over time and that the isotopic composition of the spores can also vary depending on when the cells sporulate. Based on these observations, it is conceivable that isotopic fractionation occurs during the sporulation process. Calcium, as known, forms a 1:1 chelation with dipicolinic acid (DPA) (Setlow 2006). This acid is synthesized within the mother cell and subsequently diffused in substantial quantities into the spore core during the final stages of sporulation, coinciding with the dehydration of the spore core (DPA constitutes 5 to 15% of the spore's dry weight) (Setlow 2005). Huang et al. (2007) have approximated that the concentrations of Ca-DPA in *Bacillus* species' spores exceed 800 mM, a level significantly surpassing the solubility of Ca-DPA. Notably, this acid contains carboxyl groups recognized for their ability to induce calcium fractionation (Cobert et al. 2011b; Schmitt et al. 2013). Additionally, it is plausible that fractionation occurs during Ca-DPA complex diffusion from the mother cell, its point of origin, to the spore core. Furthermore, Huang et al. (2007) have demonstrated substantial divergence in Ca-DPA levels among individual spores within a population. However, a significant portion of this variation might arise from discrepancies in individual spore sizes. Although this phenomenon likely exerts a limited impact on a substantial majority of spores, it could serve as a conceivable explanation for the divergent intensities of fractionation among the previously discussed spores.

Once sporulated, the spore pellets were rinsed and placed in contact with a Ca solution. Between 10 and 86% of Ca initially present in the solution were sorbed on the spore pellets. Spores consist of multiple layers providing considerable resistance against environmental stresses, functioning like insulating shields. Despite this robust structure, the spore envelope maintains a degree of permeability to facilitate the passage of certain molecules, including germinants, which traverse the various layers before reaching the inner membrane housing receptors (Driks 1999). Notably, molecules of modest dimensions,

like ethanol, NaOH, or HCl, can traverse the spore envelope (Setlow et al. 2002). Furthermore, the cortex, one of the deepest layers separated from the core by the inner membrane, displays a honeycomb-like structure characterized by pore sizes spanning 5–100 nm (Plomp et al. 2007). The calcium extracted from the solution can be adsorbed at varying depths within the spore, extending beyond the surface of the cortex. It's worth noting that the core of the spore is designed to maintain its dehydrated state, fortified by the impermeability conferred by the inner membrane, until the point of spore germination (Setlow 2003; Setlow et al. 2009). Given the spore's inherent nature, designed to isolate itself from the surrounding environment, no indication suggests that calcium from the solution might partially infiltrate the spore core. We cannot ascertain whether the adsorption takes place solely on the surface or if it involves diffusion through the outer envelope to reach deeper layers.

Nevertheless, similar to vegetative bacteria, neither the adsorption nor the absorption processes give rise to discernible isotopic fractionation, suggesting passive Ca sorption. Indeed, if the sorption of Ca had been accompanied by isotopic fractionation, one would expect the liquid after sorption to be enriched in the heavier isotope ^{44}Ca and the spore pellets to be enriched in the lighter isotope ^{40}Ca, which is not the case. Thus, it can be conjectured that the isotopic values found in the spores after the sorption process result from a combination of calcium originating from both the spores themselves and the remaining Ca solution from the sorption experiment in the slurry.

Utilizing a straightforward mixing equation, the proportion of calcium originating from the initial Ca sorption solution, denoted as $X(Ca)_A$, within a mixture (M) derived from two distinct sources: A (initial Ca sorption solution) and B (spore pellets) can be established in the following manner (for instance, as demonstrated in Capo et al. (1998) and Drouet et al. (2005)):

$$X(Ca)_A = \frac{\left(\Delta^{44/40}Ca\right)_M - \left(\Delta^{44/40}Ca\right)_B}{\left(\Delta^{44/40}Ca\right)_A - \left(\Delta^{44/40}Ca\right)_B} \quad (4)$$

The outcome of the mixture calculation reveals that the control primarily influences the isotopic composition of calcium. In this context, a mere 21 and 23% of the composition can be attributed to the initial calcium solution for OD_{600nm} values of 0.5 and OD_{600nm} values of 1.5, 3.5, and 4.5, respectively. As a result, regardless of the percentage of Ca sorption, approximately $21 \pm 3\%$ (N = 2, 2SD) of the Ca originates from the Ca sorption solution.

Implication for the Ca biogeochemical cycle

Biological sources and sinks of Ca during Ca cycling in forested ecosystems are of critical importance due to their significance for the carbon cycle and nutrient supply (e.g., Schmitt et al. 2012; Bullen 2014; Wiederhold 2015; Tipper et al. 2016). However, none of

Table 4 Characteristics of vegetative and sporulated bacteria, and maximum amount of adsorbed Ca and associated $^{44/40}$Ca isotopic fractionation of the supernatant measured in this study

Soil component	Grain or bacterium size (µm)	pH	Ca_{ads_max} (mmol/g)	$\Delta^{44/40}$Ca (‰)	Reference
δ-MnO_2	0.1–1	4	1.06	1.15	Schmitt et al. (2023)
δ-MnO_2	0.1–1	7	1.16	1.19	Schmitt et al. (2023)
Kaolinite (KGa-2)	0.1–1	4	4.26	0.00	Brazier et al. (2019)
Kaolinite (KGa-2)	0.1–1	7	9.66	0.00	Brazier et al. (2019)
Montmorillonite (Swy-2)	0.1–1	4	292.9	0.10	Brazier et al. (2019)
Montmorillonite (Swy-2)	0.1–1	7	293.7	0.10	Brazier et al. (2019)
Tuftane muscovite	0.1–1	4	57.95	0.22	Brazier et al. (2019)
Tuftane muscovite	0.1–1	7	63.79	0.27	Brazier et al. (2019)
Tuftane muscovite	50–200	7	0.209	0.00	Brazier et al. (2019)
Vegetative bacteria	2–4	5 to 7	< 0.1	0.00	This study
Sporulated bacteria	1	5.6	< 0.1	0.00	This study

Comparison of the data with those previously obtained in Brazier et al. (2019) for clay minerals and Schmitt et al. (2023) for δ-MnO_2

these studies have yet focused on the role of bacteria in the Ca biogeochemical cycle. Therefore, recognizing the significance of bacterial biomass and associated Ca isotope fractionation in soils is imperative. Our understanding of the microbial composition within soils remains limited. The lack of discernible fractionation during the adsorption of calcium onto bacteria does not necessarily imply the absence of any fractionation effects; rather, it may suggest that any such fractionation is too minute to be detected. Nevertheless, based on the analytical results of our study, its transposition to the natural environment would suggest the absence of isotopic fractionation associated with Ca adsorption on vegetative or spore-forming bacteria. This differs to what was previously observed for secondary soil minerals (Table 4).

The fractionation brought about by the sporulation process, despite the limited calcium quantities involved, implies that soil bacteria's sporulation/germination cycle could contribute to the isotopic signature of soil solutions. Notably, a study conducted by Siala et al. (1974) demonstrated that in coniferous forest soil, *B. subtilis* predominantly existed in vegetative form within acidic horizons, while the sporulated form prevailed in alkaline horizons. The occurrence of bacteria in either vegetative or sporulated states is governed by the prevailing environmental conditions, with multiple factors potentially influencing this phenomenon.

Accurately quantifying the proportion of bacteria existing in sporulated forms in situ might provide insight into the role of spores in shaping the isotopic composition of calcium in soil solutions. Nonetheless, limited data are presently available, and further exploration is essential to assess the potential of these research ideas. It's worth noting that the mechanism underlying sporulation can differ among various bacterial species. Despite these initial findings, the intricate nature of these mechanisms and the scarcity of data hinder a direct extrapolation of results to natural environments.

Importantly, this study concentrates on two extensively researched bacteria within laboratory settings. However, the natural environment encompasses a vast majority—over 99–99.9%—of viable yet non-cultivable bacteria. Consequently, whether the outcomes observed for these bacteria can be extended to other soil-dwelling bacterial species remains to be determined. Additionally, delving into the role of bacterial biofilms, which represent the predominant bacterial form in natural surroundings (Flemming and Wuertz 2019), as well as fungi, which generally dominate the microorganism landscape within soils (Joergensen and Wichern 2008), becomes a necessary avenue for exploration.

Conclusion

This study aimed to elucidate the direct impact of Ca adsorption of *B. subtilis* and *P. aeruginosa* and on sporulated *B. subtilis* with different surface chemical properties. The findings underscore that calcium is predominantly sequestered within bacterial cell walls of the two studied bacteria when a Ca solution interacts with bacteria. Specifically, peptidoglycan within *B. subtilis* and the outer membrane in *P. aeruginosa* are the main storage sites for Ca. Importantly, this interaction does not induce quantifiable isotopic fractionation in Ca. This observation suggests calcium primarily enters vegetative or sporulated bacteria via passive channels, allowing ^{40}Ca and ^{44}Ca isotopes to permeate. Given this absence of Ca fractionation, the process of calcium adsorption and passive incorporation onto vegetative or sporulated bacteria is unlikely to significantly influence the isotopic composition of soil solutions. However, the sporulation process stands out by inducing higher values of ^{40}Ca within spores. This variation, ranging from 0.58 to 1.20‰, is likely attributed to calcium chelation with dipicolinic acid. Consequently, the contribution of the tested vegetative and sporulated bacteria to the calcium biogeochemical cycle is merely indirect. Only the sporulation process itself fractionates Ca isotopes meaning that the impact of sporulation within soil solutions extends beyond their role in mineral bioweathering and the availability of calcium for vegetation.

Moreover, parameter variations influencing the sporulation/germination cycle can potentially lead to isotopic fluctuations in calcium within soil solutions. Subsequent investigations in macrocosms, incorporating manipulations of the germination/sporulation cycle, could validate the applicability of our findings to natural environments. It is important to note that this study exclusively focused on two planktonic bacteria. Thus, completing such study by other planktonic bacteria, as well as delving into bacterial biofilms, known for their capacity to sequester metals,

presents an intriguing avenue to further unveil the role of soil bacteria within the calcium biogeochemical cycle.

Acknowledgements Colin Fourtet, Eric Pelt and René Boutin (ITES, Strasbourg) are acknowledged for their technical assistance for the analysis. We sincerely thank the associate editor Dr. S. J. Hall as well as the anonymous reviewers for their valuable assistance in carefully proofreading our manuscript.

Funding This project was financially supported by funding from the French CNRS-INSU programme 'EC2CO-BIOHEFECT'.

Data availability The data sets generated during and/or analysed during the current study are available from the corresponding author on reasonable request.

Declarations

Competing interests The authors have no relevant financial or non-financial interests to disclose.

References

Barnes SM, Nierzwicki-Bauer SA (1997) Microbial diversity in ocean, surface and subsurface environments. Rev Mineral Geochem 35:35–79

Beveridge TJ (1999) Structures of gram-negative cell walls and their derived membrane vesicles. J Bacteriol 181:4725–4733. https://doi.org/10.1128/JB.181.16.4725-4733

Blum JD, Klaue A, Nezat CA et al (2002) Mycorrhizal weathering of apatite as an important calcium source in base-poor forest ecosystems. Nature 417:729–731. https://doi.org/10.1038/nature00793

Blum JD, Klaue A, Nezat CA et al (2003) Mycorrhizal weathering in base-poor forests. Nature 423:824–824. https://doi.org/10.1038/423824a

Braud A, Hoegy F, Jezequel K, Lebeau T, Schalk IJ (2009) New insights into the metal specificity of the *Pseudomonas aeruginosa* pyoverdine–iron uptake pathway. Environ Microbiol 11:1079–1091. https://doi.org/10.1128/JB.00010-09

Brazier JM, Schmitt AD, Gangloff S et al (2019) Calcium isotopic fractionation during adsorption onto and desorption from soil phyllosilicates (kaolinite, montmorillonite and muscovite). Geochim Cosmochim Acta 250:324–347. https://doi.org/10.1016/j.gca.2019.02.017

Brazier JM, Schmitt AD, Gangloff S et al (2020) Multi-isotope approach (δ44/40Ca, δ88/86Sr and 87Sr/86Sr) provides insights into rhizolith formation mechanisms in terrestrial sediments of Nussloch (Germany). Chem Geol 545:119641. https://doi.org/10.1016/j.chemgeo.2020.119641

Bullen TD (2014) Metal stable isotopes in weathering and hydrology. Treatise on geochemistry, 2nd edn. Elsevier, New York, pp 329–359. https://doi.org/10.1016/B978-0-08-095975-7.00511-8

Capo RC, Stewart BW, Chadwick OA (1998) Strontium isotopes as tracers of ecosystem processes: theory and methods. Geoderma 82:197–225. https://doi.org/10.1016/S0016-7061(97)00102-X

Cobert F, Schmitt AD, Bourgeade P et al (2011a) Experimental identification of Ca isotopic fractionations in higher plants. Geochimica Cosmochimica Acta 75:5467–5482. https://doi.org/10.1016/j.gca.2011.06.032

Cobert F, Schmitt AD, Calvaruso C et al (2011b) Biotic and abiotic experimental identification of bacterial influence on calcium isotopic signatures. Rapid Commun Mass Spectrom 25:2760–2768. https://doi.org/10.1002/rcm.5101

Cunrath O, Gasser V, Hoegy F et al (2015) A cell biological view of the siderophore pyochelin iron uptake pathway in *Pseudomonas aeruginosa*. Environ Microbiol 17:171–185. https://doi.org/10.1111/1462-2920.12544

Driks A (1999) *Bacillus subtilis* spore coat. Microbiol Mol Biol Rev 63:1–20. https://doi.org/10.1128/mmbr.63.1.1-20.1999

Drouet T, Herbauts J, Gruber W, Demaiffe D (2005) Strontium isotope composition as a tracer of calcium sources in two forest ecosystems in Belgium. Geoderma 126:203–223. https://doi.org/10.1016/j.geoderma.2004.09.010

Eisenhauer A, Nägler TF, Stille P, et al (2004) Proposal for international agreement on Ca notation resulting from discussions at workshops on stable isotope measurements held in davos (Goldschmidt 2002) and nice (EGS-AGU-EUG 2003). Geostand Geoanal Res 28:149–151. https://doi.org/10.1111/j.1751-908X.2004.tb01051.x

Flemming HC, Wuertz S (2019) Bacteria and archaea on Earth and their abundance in biofilms. Nat Rev Microbiol 17:247–260. https://doi.org/10.1038/s41579-019-0158-9

Futsaether CM, Johnsson A (1994) Using fura-2 to measure intracellular free calcium in *Propionibacterium acnes*. Can J Microbiol 40:439–445. https://doi.org/10.1139/m94-072

Gangloff S, Stille P, Schmitt AD, Chabaux F (2014) Impact of bacterial activity on Sr and Ca isotopic compostions ($^{87}Sr/^{86}Sr$ and $\delta^{44}/^{40}Ca$) in soil solutions (the Strengbach

CZO). Proc Earth Planet Sci 10:109–113. https://doi.org/10.1016/j.proeps.2014.08.038
Gangola P, Rosen BP (1987) Maintenance of intracellular calcium in *Escherichia coli*. J Biol Chem 262:12570–12574. https://doi.org/10.1016/S0021-9258(18)45243-X
Griffith EM, Schmitt A-D, Andrews MG, Fantle MS (2020) Elucidating modern geochemical cycles at local, regional, and global scales using calcium isotopes. Chem Geol 534:119445. https://doi.org/10.1016/j.chemgeo.2019.119445
Guillon L, El Mecherki M, Altenburger S et al (2012) High cellular organization of pyoverdine biosynthesis in *Pseudomonas aeruginosa*: clustering of PvdA at the old cell pole. Environ Microbiol 14:1982–1994. https://doi.org/10.1111/j.1462-2920.2012.02741.x
Gussone N, Schmitt AD, Heuser A et al (2016) Calcium stable isotope geochemistry. Springer, Berlin. https://doi.org/10.1007/978-3-540-68953-9
Gustafsson JP (2013) Visual MINTEQ. Version 3.1, divistion of land and water resources. Royal Institute of Technology, Stockohlm
Haferburg G, Kothe E (2007) Microbes and metals: interactions in the environment. J Basic Microbiol 47:453–467. https://doi.org/10.1002/jobm.200700275
Herbaud ML, Guiseppi A, Denizot F et al (1998) Calcium signaling in *Bacillus subtilis*. Biochim Biophys Acta Mol Cell Res 1448:212–226. https://doi.org/10.1016/S0167-4889(98)00145-1
Heuser A, Schmitt AD, Gussone N, Wombacher F (2016) Analytical methods. In: Gussone N, Schmitt AD, Heuser A et al (eds) Calcium stable isotope geochemistry. Springer, Berlin, pp 23–73
Hippler D, Schmitt A-D, Gussone N et al (2003) Calcium isotopic composition of various reference materials and seawater. Geostand Newsl 27:13–19. https://doi.org/10.1111/j.1751-908X.2003.tb00709.x
Holmden C (2005) Measurement of δ44Ca using a 42Ca-43Ca double-spike TIMS technique. Industry resources. Misc Rep 2005–1:1
Horwitz EP, McAlister DR, Bond AH, Barrans RE (2005) Novel extraction of chromatographic resins based on tetraalkyldiglycolamides: characterization and potential applications. Solvent Extr Ion Exch 23:319–344. https://doi.org/10.1081/SEI-200049898
Huang S, Chen D, Pelczar PL et al (2007) Levels of Ca^{2+}-dipicolinic acid in individual *Bacillus* spores determined using microfluidic Raman tweezers. J Bacteriol 189:4681–4687. https://doi.org/10.1128/jb.00282-07
Joergensen RG, Wichern F (2008) Quantitative assessment of the fungal contribution to microbial tissue in soil. Soil Biol Biochem 40:2977–2991. https://doi.org/10.1016/j.soilbio.2008.08.017
Jones HE, Holland IB, Baker HL, Campbell AK (1999) Slow changes in cytosolic free Ca^{2+} in *Escherichia coli* highlight two putative influx mechanisms in response to changes in extracellular calcium. Cell Calcium 25:265–274. https://doi.org/10.1054/ceca.1999.0028
Kafantaris FCA, Borrok DM (2014) Zinc isotope fractionation during surface adsorption and intracellular incorporation by bacteria. Chem Geol 366:42–51. https://doi.org/10.1016/j.chemgeo.2013.12.007
Knight MR, Campbell AK, Smith SM, Trewavas AJ (1991) Transgenic plant aequorin reports the effects of touch and cold-shock and elicitors on cytoplasmic calcium. Nature 352:524–526. https://doi.org/10.1038/352524a0
Likens GE, Driscoll CT, Buso DC et al (1998) The biogeochemistry of calcium at Hubbard Brook. Biogeochemistry 41:89–173. https://doi.org/10.1023/A:1005984620681
Lovley DR, Lloyd JR (2000) Microbes with a mettle for bioremediation. Nat Biotechnol 18:600–601. https://doi.org/10.1038/76433
Lyng M, Kovacs A (2023) Frenemies of the soil: *Bacillus* and *Pseudomonas* interspecies interactions. Trends Microbiol 31:845–857. https://doi.org/10.1016/j.tim.2023.02.003
Marschner P, Gerendás J, Sattelmacher B (1999) Effect of N concentration and N source on root colonization by *Pseudomonas fluorescens* 2–79RLI. Plant Soil 215:135–141. https://doi.org/10.1023/A:1004373007606
Matlakowska R, Skłodowska A, Nejbert K (2012) Bioweathering of Kupferschiefer black shale (Fore-Sudetic Monocline, SW Poland) by indigenous bacteria: implication for dissolution and precipitation of minerals in deep underground mine. FEMS Microbiol Ecol 81:99–110. https://doi.org/10.1111/j.1574-6941.2012.01326.x
Mulholland DS, Poitrasson F, Shirokova LS et al (2015) Iron isotope fractionation during Fe(II) and Fe(III) adsorption on cyanobacteria. Chem Geol 400:24–33. https://doi.org/10.1016/j.chemgeo.2015.01.017
Navarrete JU, Borrok DM, Viveros M, Ellzey JT (2011) Copper isotope fractionation during surface adsorption and intracellular incorporation by bacteria. Geochim Cosmochim Acta 75:784–799. https://doi.org/10.1016/j.gca.2010.11.011
Ni W, Li Y, Guan J et al (2016) Effects of efflux pump inhibitors on colistin resistance in multidrug-resistant gram-negative bacteria. Antimicrobiol Agents Chemother 60:3215–3218. https://doi.org/10.1128/AAC.00248-16
Norris V, Grant S, Freestone P et al (1996) Calcium signalling in bacteria. J Bacteriol 178:3677–3682. https://doi.org/10.1128/jb.178.13.3677-3682.1996
Ortega-Morales BO, Narváez-Zapata J, Reyes-Estebanez M et al (2016) Bioweathering potential of cultivable fungi associated with semi-arid surface microhabitats of Mayan Buildings. Front Microbiol 7:201. https://doi.org/10.3389/fmicb.2016.00201
Paidhungat M, Setlow P (2000) Role of Ger proteins in nutrient and non nutrient triggering of spore germination in *Bacillus subtilis*. J Bacteriol 182:2513–2519. https://doi.org/10.1128/jb.182.9.2513-2519.2000
Paulsen IT, Nguyen L, Sliwinski MK et al (2000) Microbial genome analyses: comparative transport capabilities in eighteen prokaryotes11Edited by G. von Heijne. J Mol Biol 301:75–100. https://doi.org/10.1006/jmbi.2000.3961
Plášek J, Babuka D, Hoefer M (2017) H+ translocation by weak acid uncouplers is independent of H+ electrochemical gradient. J Bioenerg Biomembr 49:391–397. https://doi.org/10.1007/s10863-017-9724-x
Plomp M, Leighton TJ, Wheeler KE et al (2007) In vitro high-resolution structural dynamics of single germinating bacterial spores. Proc Natl Acad Sci 104:9644–9649. https://doi.org/10.1073/pnas.0610626104

Romaniello SJ, Field MP, Smith HB et al (2015) Fully automated chromatographic purification of Sr and Ca for isotopic analysis. J Anal Spectrom 30:1906–1912

Ruas JS, Siqueira-Santos ES, Rodrigues-Silva E, Castilho RF (2018) High glycolytic activity of tumor cells leads to underestimation of electron transport system capacity when mitochondrial ATP synthase is inhibited. Sci Rep 8:17383. https://doi.org/10.1038/s41598-018-35679-8

Smith RJ (1995) Calcium and bacteria. In: Poole RK (ed) Advances in microbial physiology. Academic Press, pp 83–133

Schmitt A, Bracke G, Stille P, Kiefel B (2001) The calcium isotope composition of modern seawater determined by thermal ionisation mass spectrometry. Geostand Newsl 25:267–275. https://doi.org/10.1111/j.1751-908X.2001.tb00602.x

Schmitt A-D, Gangloff S, Cobert F et al (2009) High performance automated ion chromatography separation for Ca isotope measurements in geological and biological samples. J Anal Spectrom 24:1089–1097. https://doi.org/10.1039/B903303C

Schmitt A-D, Vigier N, Lemarchand D, Millot R, Chabaux F, Stille P (2012) Processes controlling the stable isotope compositions of Li, B, Mg and Ca in plants, soils and waters: a review. Compt Rendus Geosci 344:704–722

Schmitt AD, Cobert F, Bourgeade P et al (2013) Calcium isotope fractionation during plant growth under a limited nutrient supply. Geochim Cosmochim Acta 110:70–83. https://doi.org/10.1016/j.gca.2013.02.002

Schmitt AD, Gangloff S, Labolle F et al (2017) Calcium biogeochemical cycle at the beech tree-soil solution interface from the Strengbach CZO (NE France): insights from stable Ca and radiogenic Sr isotopes. Geochim Cosmochim Acta 213:91–109. https://doi.org/10.1016/j.gca.2017.06.039

Schmitt AD, Gangloff S, Brazier JM et al (2023) Calcium isotope fractionation associated with adsorption and desorption on/from δ-MnO2. Geochim Cosmochim Acta 354:109–122. https://doi.org/10.1016/j.gca.2023.06.003

Setlow B, Atluri S, Kitchel R et al (2006) Role of dipicolinic acid in resistance and stability of spores of *Bacillus subtilis* with or without DNA-protective α/β-type small acid-soluble proteins. J Bacteriol 188:3740–3747. https://doi.org/10.1128/JB.00212-06

Setlow B, Loshon CA, Genest PC et al (2002) Mechanisms of killing spores of *Bacillus subtilis* by acid, alkali and ethanol. J Appl Microbiol 92:362–375. https://doi.org/10.1046/j.1365-2672.2002.01540.x

Setlow B, Peng L, Loshon CA et al (2009) Characterization of the germination of *Bacillus megaterium* spores lacking enzymes that degrade the spore cortex. J Appl Microbiol 107:318–328. https://doi.org/10.1111/j.1365-2672.2009.04210.x

Setlow P (2006) Spores of *Bacillus subtilis*: their resistance to and killing by radiation, heat and chemicals. J Appl Microbiol 101:514–525. https://doi.org/10.1111/j.1365-2672.2005.02736.x

Setlow P (2003) Spore germination. Curr Opin Microbiol 6:550–556. https://doi.org/10.1016/j.mib.2003.10.001

Setlow P (2005) The bacterial spore: nature's survival package. Culture 26:1–8

Shabtai IA, Wilhelm RC, Schweitzer SA, Höschen C, Buckley DH, Lehmann J (2023) Calcium promotes persistent soil organic matter by altering microbial transformation of plant litter. Nat Commun 14:6609. https://doi.org/10.1038/s41467-0.23-42291-6

Siala A, Hill IR, Gray TRG (1974) Populations of spore-forming bacteria in an acid forest soil, with special reference to *Bacillus subtilis*. Microbiology 81:183–190. https://doi.org/10.1099/00221287-81-1-183

Spiers AJ, Buckling A, Rainey P (2000) The causes of *Pseudomonas* diversity. Microbiology 146:2345–2350. https://doi.org/10.1099/00221287-146-10-2345

Tipper ET, Schmitt AD, Gussone N (2016) Global Ca cycles: coupling of continental and oceanic processes. In: Gussone N, Schmitt AD, Heuser A, Wombacher F, Dietzel M, Tipper E, Schiller M (eds) Calcium stable isotope geochemistry. Springer, Cham, pp 173–222

Torrecilla I, Leganés F, Bonilla I, Fernández-Piñas F (2000) Use of recombinant aequorin to study calcium homeostasis and monitor calcium transients in response to heat and cold shock in cyanobacteria1. Plant Physiol 123:161–176. https://doi.org/10.1104/pp.123.1.161

Vanmechelen L, Groenemans R, Van Ranst E (1997) Forest soil condition in Europe. Forest Soil Co-ordinating Centre, International Co-operative Programme on Assessment and Monitoring of Air Pollution on Forest, UN-ECE. p 35

Waditee R, Hossain GS, Tanaka Y et al (2004) Isolation and functional characterization of Ca^{2+}/H^{+} antiporters from cyanobacteria. J Biol Chem 279:4330–4338. https://doi.org/10.1074/jbc.M310282200

Wasylenki LE, Anbar AD, Liermann LJ et al (2007) Isotope fractionation during microbial metal uptake measured by MC-ICP-MS. J Anal Spectrom 22:905. https://doi.org/10.1039/b705476a

Wiederhold JG (2015) Metal stable isotope signatures as tracers in environmental geochemistry. Environ Sci Technol 49:2606–2624

Zhang Q, Amor K, Galer SJG et al (2018) Variations of stable isotope fractionation during bacterial chromium reduction processes and their implications. Chem Geol 481:155–164. https://doi.org/10.1016/j.chemgeo.2018.02.004